Tim Stauch

A mechanochemical model for the simulation of molecules and molecular crystals under hydrostatic pressure

Recommended Citation (primary publication/Version of Record) incl. DOI:

Tim Stauch; A mechanochemical model for the simulation of molecules and molecular crystals under hydrostatic pressure. J. Chem. Phys. 7 October 2020; 153 (13): 134503. https://doi.org/10.1063/5.0024671

Take down policy

Tim Stauch (iD)

View Online

Export Citation

CrossMark

The Journal of Chemical Physics

AIP Publishing

A mechanochemical model for the simulation of molecules and molecular crystals under hydrostatic pressure

View Online   Export Citation   CrossMark

Tim Stauch[a] (iD)

AFFILIATIONS

University of Bremen, Institute for Physical and Theoretical Chemistry, Leobener Straße NW2, D-28359 Bremen, Germany;
Bremen Center for Computational Materials Science, University of Bremen, Am Fallturm 1, D-28359 Bremen, Germany;
and MAPEX Center for Materials and Processes, University of Bremen, Bibliothekstraße 1, D-28359 Bremen, Germany

[a]Author to whom correspondence should be addressed: tstauch@uni-bremen.de

ABSTRACT

A novel mechanochemical method for the simulation of molecules and molecular crystals under hydrostatic pressure, the *eXtended Hydro-static Compression Force Field* (X-HCFF) approach, is introduced. In contrast to comparable methods, the desired pressure can be adjusted non-iteratively and molecules of general shape retain chemically reasonable geometries even at high pressure. The implementation of the X-HCFF approach is straightforward, and the computational cost is practically the same as for regular geometry optimization. Pressure can be applied by using any desired electronic structure method for which a nuclear gradient is available. The results of the X-HCFF for pressure-dependent intramolecular structural changes in the investigated molecules and molecular crystals as well as a simple pressure-induced dimerization reaction are chemically intuitive and fall within the range of other established computational methods. Experimental spectroscopic data of a molecular crystal under pressure are reproduced accurately.

Published under license by AIP Publishing. https://doi.org/10.1063/5.0024671

I. INTRODUCTION

The field of high-pressure chemistry has seen tremendous progress within the past few decades.[1] Pressure-induced changes in the rate, mechanism, and equilibrium of chemical reactions have opened up new avenues in chemical synthesis.[2,3] Using diamond-anvil cells,[4] pressures of several hundred GPa have been realized experimentally, meaning that pressures as high as in the Earth's core are now available in the laboratory.[5] Not surprisingly, the geometries of molecules,[6–8] the lattice constants of crystals,[9–12] and crystal phases[13,14] have been found to change under pressure. However, many of the pressure-induced structural changes of molecules and crystals can only be inferred indirectly by interpreting the concomitant changes in the spectroscopic properties, e.g., the wavelengths and intensities of absorption.

As a result, the demand for computational tools that predict structural and spectroscopic properties of molecules as well as chemical reactivity at high pressure is increasing. Methods that model the influence of pressure on periodic chemical systems have been described in the realm of molecular dynamics[13,15] and *ab initio* molecular dynamics (AIMD).[16–18] At the single-molecule level, several electronic structure methods for the simulation of molecules under pressure are available.[19] A particularly notable example is the *eXtreme Pressure Polarizable Continuum Model* (XP-PCM),[20–22] in which pressure is applied to an atom or a molecule via a surrounding medium. In the XP-PCM, pressure is modeled by decreasing the size of the cavity inside which the system is placed and simultaneously increasing the Pauli repulsion of the surrounding medium. The XP-PCM has been used, e.g., in the simulation of chemical reactions[21–23] and for investigating changes in spectroscopic,[24,25] electronic,[26] and structural[27] properties of atoms and molecules under pressure.

A straightforward alternative to model molecules under pressure has its roots in quantum mechanochemistry.[28] The earliest quantum mechanochemical method for the application of pressure is the *Generalized Force-Modified Potential Energy Surface*

(G-FMPES) model,[29–31] which builds on the FMPES scheme,[32] a protocol to optimize molecular geometries under external forces. In the G-FMPES, mechanical forces compress a molecule toward its geometric centroid during geometry optimization. A variation of this method, the *Hydrostatic Compression Force Field* (HCFF) approach,[33] differs from the G-FMPES mainly in the definition of the surface area and the calculation of the pressure that is applied to the molecule. The HCFF has been used to calculate the pressure required to trigger spin-crossover in octahedral metal–ligand complexes.[33] A drawback of the quantum mechanochemical pressure models, however, is that the pressure that is applied to the molecule cannot be defined *a priori*. Instead, the applied pressure is calculated from empirical parameters that are specified by the user, meaning that the desired pressure has to be adjusted iteratively. A second drawback is that in some cases, e.g., in extended molecules, unreasonable molecular geometries are found by the G-FMPES and HCFF due to the tendency of the molecule to minimize its surface area under compression. Hence, both the G-FMPES and the HCFF work the best for molecules that can be approximated as spherical.

In this paper, a new member of the family of mechanochemical pressure models, the *eXtended Hydrostatic Compression Force Field* (X-HCFF), is presented. It builds on the HCFF approach but avoids the deficiencies of the previous mechanochemical pressure models in that (1) the user has full control over the pressure that is applied to the molecule and (2) the pressure is applied truly hydrostatically, i.e., the compression of extended molecules can be simulated realistically. It is shown that structural parameters calculated with the novel X-HCFF model are of the same quality of those calculated with previous computational methods in both single molecules and molecular crystals and that experimental spectroscopic parameters can be reproduced accurately in the investigated test systems. Moreover, a pressure-induced chemical reaction is reproduced. The implementation of the X-HCFF approach is straightforward and only requires a surface tessellation routine, which is typically implemented in connection with implicit solvent models in many quantum chemical program packages, as well as a nuclear gradient code for the desired electronic structure method. While the calculations presented in this paper were all carried out with Density Functional Theory (DFT),[34,35] wave-function based methods can of course be used instead. The computational cost of an X-HCFF calculation is virtually identical to the cost of regular, pressure-free geometry optimization. The X-HCFF model will be available in a future release of the Q-Chem program package.[36]

The rest of this paper is structured as follows: After establishing the theoretical foundation of the X-HCFF approach in Sec. II, the performance of the method is tested in Sec. III. In particular, comparisons are made against structural parameters of molecules under pressure calculated with the HCFF (Sec. III A) and XP-PCM (Sec. III B). The performance of the X-HCFF for the description of molecular crystals under pressure is tested by comparing against results calculated with periodic DFT (Sec. III C) as well as against experimental Raman spectra under pressure (Sec. III D). Finally, the dimerization of carbon dioxide under pressure is investigated in (Sec. III E) to demonstrate the capability of the X-HCFF to describe a simple pressure-induced chemical reaction. Possible routes for future developments are pointed out in Sec. IV.

II. THEORY

A. Theoretical background of HCFF

As the X-HCFF is based on the HCFF approach, the theoretical background of the latter shall be summarized first. In the HCFF, mechanical forces pointing toward the non-mass-weighted molecular centroid are applied on the nuclei to compress a molecule.[33] As motivated in the literature for the closely related G-FMPES approach,[29–31] the force acting on each atom is potentially unique, with the largest force acting on the outermost atom and the forces on the inner atoms being scaled by the distances of these atoms to the geometric centroid of the system. Using this condition as well as the definition of the pressure, $P = F_\perp/A$, where $F_\perp$ is the normal component of the force at the surface and A is the surface area, the magnitude of the force f_i^{HCFF} pushing an atom i toward the molecular centroid is calculated in the HCFF scheme as

$$|f_i^{\text{HCFF}}| = -P_{\text{guess}} \cdot A_{\text{vdW}} \cdot \frac{r_i}{r_{\text{max}}}, \qquad (1)$$

where P_{guess} is a user-defined guess for the pressure that is applied to the molecule, A_{vdW} is the molecular van der Waals surface area, r_i is the distance of the atom i to the molecular centroid, and r_{max} is the distance of the outermost atom to the centroid. The van der Waals surface is used as the definition of the molecular surface, since the surrounding medium, which applies pressure to the molecule, e.g., in a diamond-anvil cell, is in contact with the molecule at its van der Waals surface. The forces f_i^{HCFF} are then added to the nuclear gradient during geometry optimization, leading to compression of the molecule. As in other quantum mechanochemical optimization techniques,[37] the optimization converges if the externally applied force (in this case all forces f_i^{HCFF}) and the internal restoring forces cancel. The pressure acting on the molecule has to be calculated *a posteriori* via

$$P_{\text{HCFF}} = \frac{\langle \|f\| \rangle}{A_{\text{vdW}}}, \qquad (2)$$

where $\langle \|f\| \rangle$ is the average force acting on the atoms. Typically, P_{guess} overestimates P_{HCFF}. Hence, the pressure that is applied to the molecule cannot be specified directly and instead needs to be calculated from a user-defined parameter, which is one of the major drawbacks of the mechanochemical models of pressure that have been developed. Moreover, since the forces are acting toward the molecular centroid, molecules tend to minimize their surface areas. As a result, unreasonable compressed geometries can ensue[33] and extended molecules can fold into sphere-like objects, which is not the expected behavior in hydrostatic compression experiments.

B. The X-HCFF approach

Both problems are circumvented in the X-HCFF approach. The basic idea that pressure is mediated to the molecule via its van der Waals surface, e.g., during hydrostatic compression in a diamond-anvil cell, is carried over from the HCFF to the X-HCFF. In many quantum chemical program packages, the van der Waals surface is calculated by superimposing atom-centered spheres, removing the overlapping regions and tessellating the surface using a Lebedev grid [Fig. 1(a)].[38] Instead of compressing the molecule toward its centroid, in the X-HCFF, truly hydrostatic compression is achieved

A

B
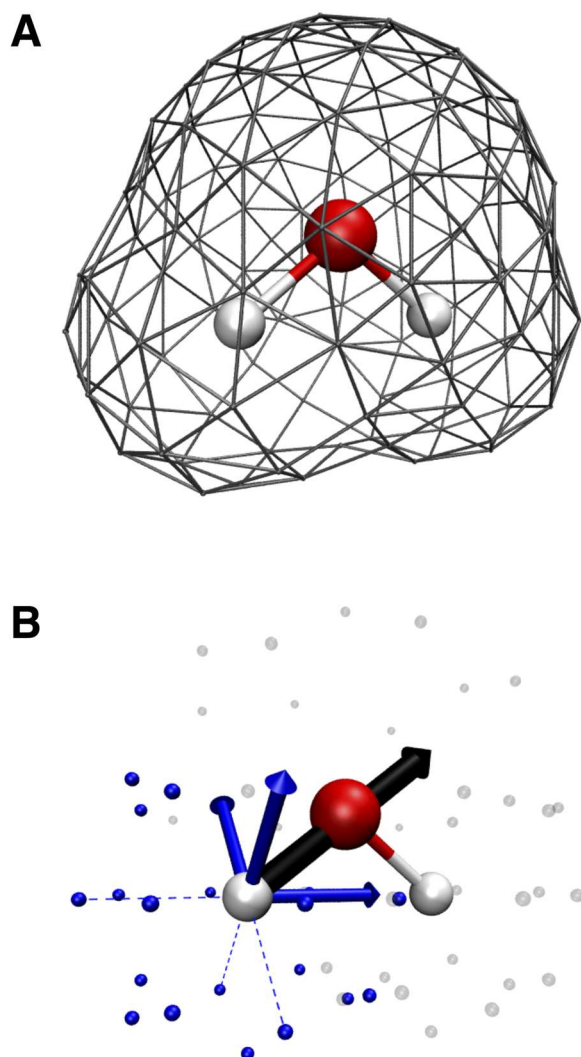
FIG. 1. (a) van der Waals surface of the water molecule approximated by a Lebedev grid, leading to a tessellated surface. (b) Basic idea of the X-HCFF approach for the water molecule with a reduced number of tessellation points, taking one of the hydrogen atoms as an example. The blue spheres represent the tessellation points created by the van der Waals sphere around the hydrogen atom under consideration, whereas the transparent spheres are the tessellation points associated with the other atoms in the molecule. Dotted lines connect the tessellation points to the hydrogen atom, and the blue arrows depict the resulting gradient contributions. For clarity, the force contributions of only three tessellation points are shown. The thick black arrow represents the resulting force that arises when adding up each individual gradient contribution for the hydrogen atom. Arrows are not drawn to scale.

by applying the forces perpendicular to the van der Waals surface at each tessellation point [Fig. 1(b)].

Each surface tessera j has an area A_j, and the van der Waals surface is calculated as $A_{vdW} = \sum_j^{N_{Tess}} A_j$, where N_{Tess} is the number of tessellation points. In the X-HCFF, the force $\mathbf{f}_{i,j}$ acting on the atom i that stems from the pressure on the surface tessera j acts along the

connecting line between the atom i and the tessera j and points away from the latter [blue arrows in Fig. 1(b)]. Using again the definition of pressure, this force can be calculated via

$$\mathbf{f}_{i,j} = -P \cdot A_j \cdot \frac{(\mathbf{r}_i - \mathbf{r}_j)}{|\mathbf{r}_i - \mathbf{r}_j|}, \qquad (3)$$

where P is the pressure that is applied to the molecule, $\mathbf{r}_i$ is the position of the atom i, and $\mathbf{r}_j$ is the position of the tessera j. The net force acting on the atom i is then calculated by summing up the contributions from each surface tessera that lies on the van der Waals sphere around the atom i [blue spheres in Fig. 1(b)],

$$\mathbf{f}_i = \sum_j^{N_{Tess},i} \mathbf{f}_{i,j}. \qquad (4)$$

When calculating the gradient contribution for an atom, the tesserae that lie on the van der Waals spheres around the other atoms are ignored. Since the force contributions from tesserae on opposite sides of the atom cancel and there are no tessellation points along the connecting line between two atoms, the resulting force contribution pushes the atoms toward one another, leading to compression of the molecule. The forces calculated for each atom via Eq. (4) are added to the nuclear gradient during geometry optimization, which converges when the external force due to pressure and the internal restoring force of the molecule cancel. Since the tessellation is carried out anew in each optimization step, the tessellation field reacts to the updated molecular geometry. As a result, the forces applied to the atoms are adjusted each time such that the input pressure P is applied to the molecule. However, the X-HCFF ansatz does not strictly guarantee that the gradient contributions on all atoms add up to zero in all cases, which is required to prevent translation and rotation of the molecule. While in all investigated systems the resulting net gradient contribution was extremely small, it was split up evenly and added to the nuclear gradient of each atom.

For the *a priori* definition of the pressure, it is crucial to pick a specific scaling factor of the van der Waals radii. In implicit solvent models, a scaling factor of 1.2 is commonly applied to the van der Waals radii to account for the intrinsic distance between the solvent molecules and the solute.[38] However, it has been found that the van der Waals radii decrease upon application of pressure,[39] which can be traced back to the compression of the electron density that is not described by the mechanochemical models of pressure. As a compromise, the unscaled van der Waals radii by Bondi[40] are used in the X-HCFF approach. Since upon application of pressure the van der Waals radii decrease with a slope that is individual for each atom[39] and the resulting differences in compressibility of different atoms have an impact on the geometries, the X-HCFF will likely be the basis for more sophisticated pressure models that include the compression of the electron density to lead to a more realistic description of chemical systems under pressure. Beneficially, however, the only remaining parameter in the X-HCFF model is the number of tessellation points per atom. The dependence of the results on this parameter is tested in Sec. III B.

It should be pointed out that the scope of the mechanochemical models of pressure, including the X-HCFF, is limited to molecules, since the utilization of the nuclear gradient precludes the treatment of atoms. This can, however, be achieved with the XP-PCM

approach[20–22] and was indeed used in the past to determine the electronic configuration of atoms under pressure.[26,39]

III. RESULTS AND DISCUSSION

A. Comparison between X-HCFF and HCFF

To showcase the difference between the X-HCFF and the HCFF, an aliphatic molecule is compressed using both approaches. While the HCFF was shown to deliver physically meaningful and chemically intuitive results for molecules that can be circumscribed onto a sphere,[33] the method performs poorly for butane under a pressure of 50 GPa (Fig. 2): Since strong forces point toward the molecular centroid and these forces are strongest for the outermost atoms, the molecule tends to minimize its surface and folds into a sphere-like object. This situation is reminiscent of planets and stars, in which gravitational forces pull each particle toward the center, resulting in (roughly) spherical shapes. The creation of a sphere-like geometry is a general feature of the HCFF and can also be observed in many other molecules, which limits the applicability of the method. In the present case, this leads to SCF convergence failure. Moreover, the applied pressure is smaller than the initially chosen value [cf. Eqs. (1) and (2)], thus preventing the *a priori* adjustment of the desired pressure.

The X-HCFF approach, on the other hand, is not afflicted with these disadvantageous features. While the bond lengths in the molecules are shortened by pressure and bond angles change (cf. the supplementary material, Tables S1 and S2), the extended shape of butane is retained at 50 GPa (Fig. 2). This is due to the fact that each atom is being pushed inward orthogonally to the surface, leading to compression of the covalent bonds and not to the creation of a sphere-like geometry. Therefore, the X-HCFF is more generally
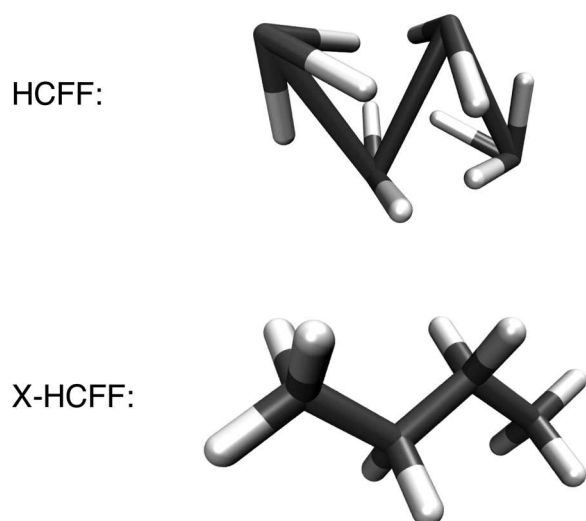
applicable for the simulation of molecules under hydrostatic pressure than the HCFF.

B. Structural parameters in *trans*-1,3-butadiene as a function of pressure

To judge the dependence of structural data calculated with the X-HCFF on the number of tessellation points, *trans*-1,3-butadiene is used as a test case. Here, values between 6 and 1202 tessellation points per atom are adjusted. Focusing on the central carbon–carbon bond length in *trans*-1,3-butadiene, it can be observed that with the exception of the smallest number of tessellation points, the results converge quickly (Fig. 3). With the increasing pressure, the bond length decreases with the same slope for all values between 26 and 1202 tessellation points per atom. Similar results were obtained for all other investigated systems during testing. This is a profitable feature of the X-HCFF because the number of tessellation points is the only empirical parameter in the model and the results are virtually independent of the precise choice of this parameter. As the cost of the calculation is influenced only insignificantly by the number of tessellation points per atom, a value of 302 is used in the remainder of this paper.

Since *trans*-1,3-butadiene was treated previously with the XP-PCM,[20] this molecule provides a testing ground for the performance of the X-HCFF in comparison with another computational method for the simulation of molecules under pressure. Comparing the bond lengths in *trans*-1,3-butadiene calculated with the XP-PCM and X-HCFF (Fig. 4), it becomes apparent that the pressure-induced decrease in carbon–carbon bond lengths is more pronounced in the X-HCFF than in the XP-PCM. In addition, the X-HCFF curve for the central carbon–carbon bond is smoother than that in the XP-PCM. In agreement with chemical intuition, the X-HCFF predicts a significantly higher compressibility of the central carbon–carbon bond compared to the terminal carbon–carbon bonds, due to the lower double bond character and the accompanying lower force constant of the former. Hence, the X-HCFF offers the possibility to calculate the structural changes induced by pressure reliably, which

FIG. 2. Molecular geometries for butane at a pressure of 50 GPa as calculated with the HCFF[33] (top; shortly before convergence failure) and X-HCFF (bottom) approaches at the PBE[41]/cc-pVDZ[42] level of theory with 302 tessellation points for each atom.
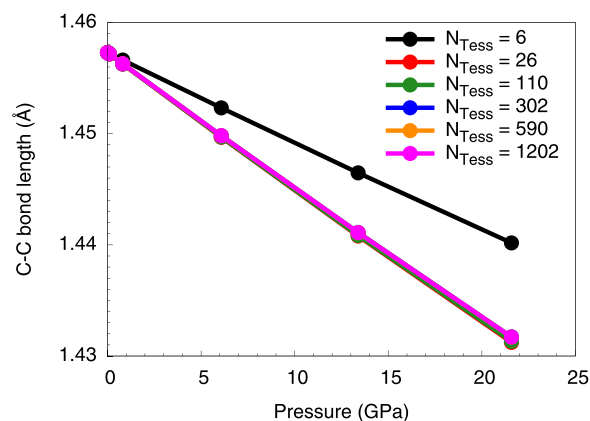
FIG. 3. Dependence of the central C–C bond length in *trans*-1,3-butadiene on the number of tessellation points (N_{Tess}) per atom, calculated with the X-HCFF at the B3LYP[43–45]/6-31G(d,p)[46] level of theory.
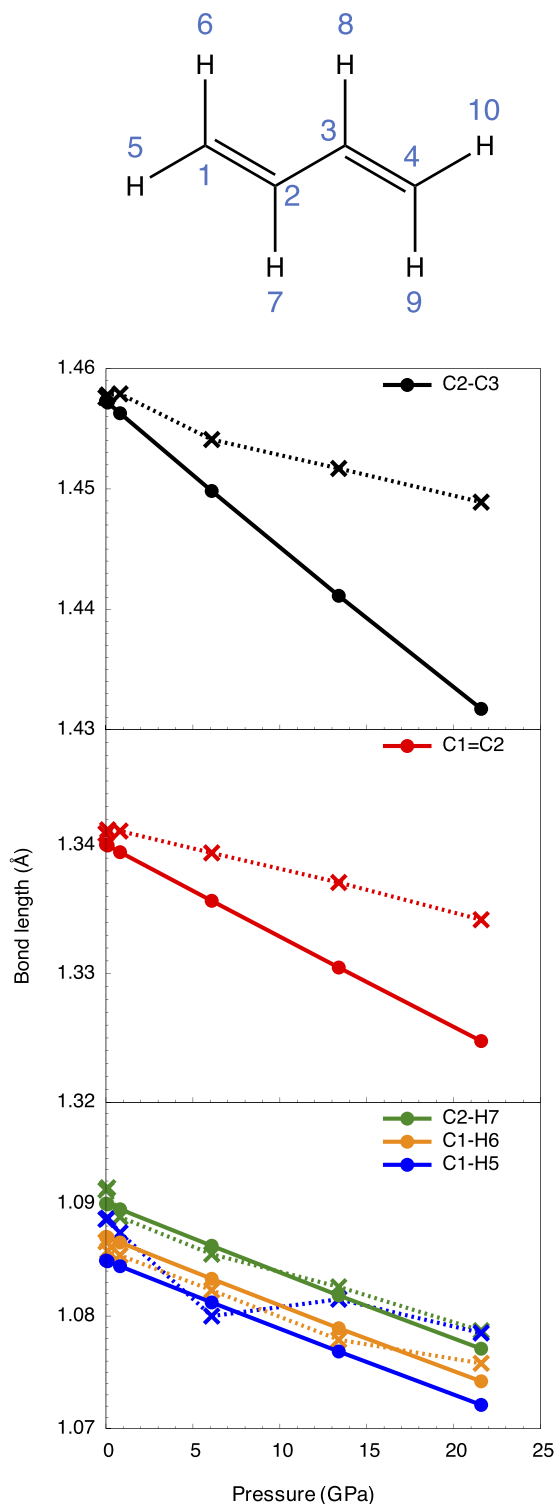
FIG. 4. Bond lengths in *trans*-1,3-butadiene at different pressures. Circles connected by solid lines denote the X-HCFF results. Crosses connected by dotted lines represent literature values (Ref. 20), calculated with the XP-PCM. In both cases, B3LYP/6-31G(d,p) was taken as the electronic structure method.

is traditionally considered a challenging task due to the scarcity of available computational models.[9] Turning to the carbon–hydrogen bond lengths, the results of the X-HCFF and XP-PCM are more similar, with the difference that the bond lengths calculated with the X-HCFF again decrease more smoothly. In particular, the X-HCFF finds a monotonic decrease in one of the terminal carbon–hydrogen bond lengths (C1–H5 in Fig. 4), while this is not the case for the XP-PCM.

A comparison between the X-HCFF and the HCFF in the case of *trans*-1,3-butadiene can be found in the supplementary material (Figs. S1 and S2). As in the case of butane (Sec. III A), the HCFF delivers unphysical geometries at high pressure. In addition, the decrease in bond lengths under pressure calculated with the HCFF is up to an order of magnitude more pronounced than in the X-HCFF and shows non-monotonic behavior. Since the HCFF and G-FMPES differ mainly in the definition of the surface area, it can be seen that the X-HCFF outperforms the previous mechanochemical models of pressure also in the case of *trans*-1,3-butadiene. Further comparisons between the X-HCFF and previous mechanochemical pressure models are refrained from in the remaining part of this paper.

These results demonstrate that using a single *trans*-1,3-butadiene molecule as an example, the X-HCFF affords continuous curves showing the progressive decrease in bond lengths with the increasing pressure, in agreement with chemical intuition, and that the decrease in bond lengths is proportional to the external pressure. Extensive test calculations on a wide variety of molecules need to be carried out to judge how general this trend is.

C. Structural parameters in a molecular crystal as a function of pressure

The performance of the X-HCFF when treating molecular crystals is tested by calculating structural parameters of 7-nitrotetrazolo [1,5]furazano[4,5-b]pyridine 1-oxide (NFP), for which reference values calculated with a periodic implementation of DFT are available.[47] The focus of the present study lies on intramolecular geometric changes and not on changes in the lattice parameters, so that a single NFP molecule is subjected to pressures between 0 GPa and 100 GPa with the X-HCFF model. As can be seen in Fig. 5, the X-HCFF results can compete with those obtained via periodic DFT. Despite the differences in the approaches and the applied electronic structure levels, which lead to deviations in the bond lengths at 0 GPa, many of the bond lengths in NFP decrease with roughly the same slope in both approaches. Notable differences include the bond lengths N10–N12 and N8–O14, which remain almost constant and even increase occasionally in the periodic calculations, whereas they decrease monotonically in the X-HCFF. It can be hypothesized that these differences can be traced back to crystal packing effects that are not captured by the X-HCFF. However, one can state that the structural parameters calculated with the X-HCFF for the molecular NFP crystal are chemically intuitive, and for many bond lengths, the agreement with periodic calculations is remarkable, which is an encouraging result considering that only a single molecule is treated with the X-HCFF. Nevertheless, in the future, a careful calibration of the size of the system investigated with the X-HCFF, i.e., the number of molecules subjected to pressure in the geometry optimization, needs to be carried out to determine the influence of the chemical

NFP
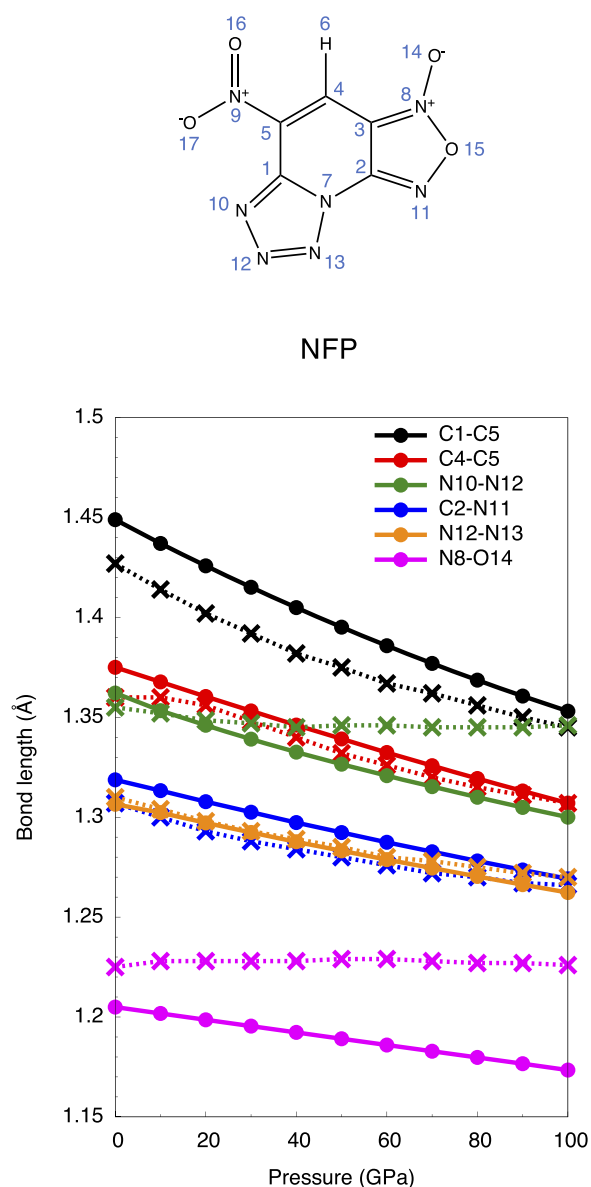
FIG. 5. Selected bond lengths in NFP at different pressures. Circles connected by solid lines denote the X-HCFF values, calculated with PBE/cc-pVDZ. Crosses connected by dotted lines represent literature values (estimated graphically from Ref. 47), calculated with Density Functional Theory (DFT) for periodic systems.

environment in the crystal on the structural parameters of an individual molecule.

D. Comparison with experimental Raman spectra under pressure

Although comparisons of structural data of single molecules and molecular crystals calculated with the X-HCFF and other approaches are helpful to judge the performance of the new method,

the clearest criterion for its reliability is the direct comparison with experimental data. Experimental structural data of molecules and crystals under pressure are typically inferred from spectroscopic observables. A notable example is the pressure-induced increase in the wavenumber of the Raman-active C–H stretching vibration in the molecular crystal 2-amine-1,3,4-thiadiazole (ATD), which has been reported recently.[48] It was found that the wavenumber of this vibration in the ATD crystal increases linearly with the increasing pressure.

Applying the same pressures as in the experiments to ATD with the X-HCFF approach at the PBE/cc-pVDZ level of theory and subsequently calculating the Raman spectra yield virtually identical changes in the Raman spectrum (Fig. 6), provided that the calculated wavenumbers are scaled with the ratio between the experimental (3096 cm^{-1}) and the calculated (3171 cm^{-1}) signal at 0 GPa. The full set of scaled and unscaled calculated wavenumbers of the Raman-active C–H stretching vibration in ATD at different pressures can be found in the supplementary material (Table S4). Since experiments are free from the approximations made in other approaches for the simulation of molecules under pressure to which the X-HCFF was compared in Secs. III A–III C, the accurate reproduction of the experimental spectroscopic data presented here emphasizes the usefulness of the X-HCFF in the simulation of chemical systems under pressure. The results suggest that both the experimental geometric changes and the accompanying response of the Raman spectra of the ATD crystal are captured accurately by the X-HCFF.

ATD
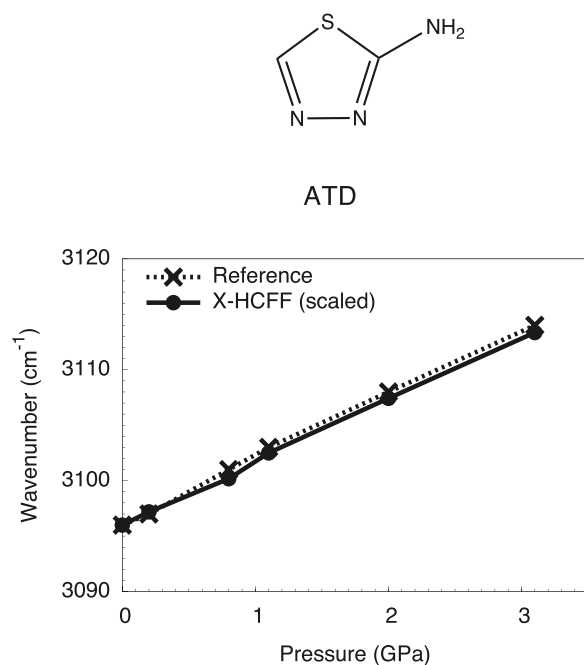
FIG. 6. Wavenumbers of the Raman-active C–H stretching vibration in ATD at different pressures, calculated with the X-HCFF at the PBE/cc-pVDZ level of theory. The maxima of the peaks in the experimental Raman spectra presented in Ref. 48 were taken as the reference values. The X-HCFF values were scaled such that the experimental and calculated peaks at 0 GPa coincide.

E. Pressure-induced dimerization of carbon dioxide

To test the applicability of the X-HCFF approach when describing pressure-induced chemical reactions, the dimerization of carbon dioxide under pressure is investigated as an example. This reaction has been described previously using *ab initio* molecular dynamics (AIMD) simulations[49] and has been proposed as an intermediate step in the formation of polymeric CO_2 under pressure.

Starting with a van der Waals complex of two CO_2 molecules with a lateral distance of 3.15 Å between each other, the application of pressure with the X-HCFF at the PBE/cc-pVDZ level of theory leads to a continuous decrease in the distance between the two CO_2 molecules up to 90 GPa (Fig. 7). Between 90 GPa and 100 GPa, the distance between the CO_2 molecules decreases sharply, marking the formation of covalent bonds in the resulting CO_2 dimer. A further increase in pressure leads to only a minor compression of the C–O bonds within the four-membered ring of the CO_2 dimer. Interestingly, carrying out pressure-free geometry optimization using the CO_2 dimer created at 100 GPa as an input structure, the dimeric geometry is retained, emphasizing the metastable nature of the dimer that was described previously.[49] However, in the AIMD simulations, the CO_2 dimer was observed as a short-lived species at pressures of 20 GPa and 50 GPa, which is lower than that in the X-HCFF calculations. A possible reason for the higher pressure required to form the CO_2 dimer using the X-HCFF is that in contrast to AIMD simulations, thermal oscillations are not taken into account. Such fluctuations, however, lead to molecular oscillations and could deliver crucial energy required to overcome the reaction barrier. Similar effects have been discussed as the reason for the overestimation of rupture forces by static quantum chemical methods when describing mechanochemical processes.[28] Detailed calculations will need to be carried out to reliably compare the pressures required to induce chemical reactions calculated by dynamic and static simulation techniques.

The pressure-induced dimerization of CO_2, which was successfully described with the X-HCFF, demonstrates that the predictive power of the new method is not limited to pressure-dependent structural and spectroscopic properties but also has high potential in describing chemical reactions under pressure. In this case, a minimum on the potential energy surface under pressure, which was revealed by previous AIMD simulations, could be reproduced at the computational cost of a quantum chemical geometry optimization.
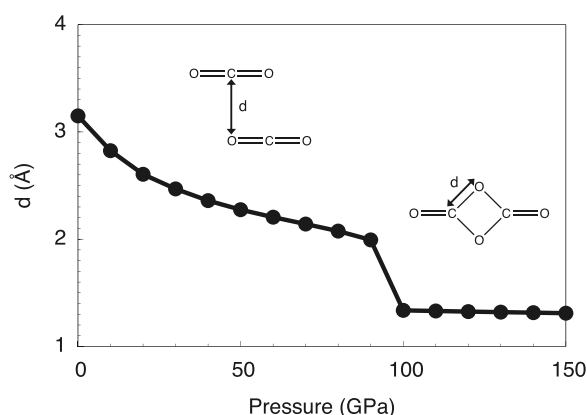
IV. CONCLUSIONS AND OUTLOOK

In this paper, the *eXtended Hydrostatic Compression Force Field* (X-HCFF), a novel mechanochemical method for the simulation of molecules and molecular crystals under hydrostatic pressure, was introduced. The X-HCFF method avoids common problems of related approaches and accurately reproduces computational and experimental structural and spectroscopic reference data in a variety of test systems. The straightforward implementation and the user-friendly and inexpensive computation make the X-HCFF a useful method for calculations of structural and spectroscopic properties as well as chemical transformations of molecules and molecular crystals under hydrostatic pressure.

In the future, careful benchmarks of various density functionals and wave-function based methods will be carried out to determine the optimal electronic structure method that reproduces experimental structural and spectroscopic data most accurately. Moreover, it is planned to leave the realm of small test systems and evaluate the applicability of the X-HCFF when treating crystallites. A particularly interesting question is whether pressure-induced changes in lattice constants[10–12] can be reproduced by using a quantum mechanochemical method. The ability of the X-HCFF to go beyond the treatment of single molecules and deliver chemically meaningful results for the dimerization of carbon dioxide is very promising in this regard. Another future route is provided by AIMD simulations, with which the X-HCFF can be combined easily, to simulate the time evolution of structural changes of molecules under pressure. This will be particularly useful in modeling pressure-induced adsorption and desorption processes of, e.g., industrially relevant gases on surfaces. Furthermore, more complex chemical reactions under pressure, e.g., Diels–Alder reactions, will be treated with the X-HCFF in the future.

Finally, it is important to note that in the X-HCFF approach, molecules react toward hydrostatic pressure only through force-induced compression of the nuclear scaffold. While this opens up the interesting possibility of relating the strain induced by the compression with chemical reactivity,[50] one must acknowledge that in X-HCFF pressure does not interact directly with the electrons, but only indirectly through an altered arrangement of the nuclei. A computational method that simulates the influence of pressure on molecules via interactions with the electron density is currently under development.

SUPPLEMENTARY MATERIAL

See the supplementary material for structural data for butane calculated with the X-HCFF; structural data for *trans*-1,3-butadiene calculated with the X-HCFF and HCFF; Raman signals in ATD calculated with the X-HCFF; and initial geometry of the carbon dioxide dimer.

FIG. 7. Distance *d* between the carbon atom of a CO_2 molecule and an oxygen atom of another CO_2 molecule as a function of pressure, using the X-HCFF at the PBE/cc-pVDZ level of theory. After dimerization occurs at ~100 GPa, *d* denotes the C–O bond length in the four-membered ring of the CO_2 dimer.

DATA AVAILABILITY

The data that support the findings of this study are available from the author upon reasonable request.

REFERENCES

[1] P. F. McMillan, "Chemistry at high pressure," Chem. Soc. Rev. **35**, 855–857 (2006).

[2] W. Grochala, R. Hoffmann, J. Feng, and N. W. Ashcroft, "The chemical imagination at work in very tight places," Angew. Chem., Int. Ed. **46**, 3620–3642 (2007).

[3] V. Schettino and R. Bini, "Constraining molecules at the closest approach: Chemistry at high pressure," Chem. Soc. Rev. **36**, 869–880 (2007).

[4] B. Li, C. Ji, W. Yang, J. Wang, K. Yang, R. Xu, W. Liu, Z. Cai, J. Chen, and H.-k. Mao, "Diamond anvil cell behavior up to 4 Mbar," Proc. Natl. Acad. Sci. U. S. A. **115**, 1713–1717 (2018).

[5] L. Stixrude and R. E. Cohen, "High-pressure elasticity of iron and anisotropy of Earth's inner core," Science **267**, 1972–1975 (1995).

[6] N. Casati, A. Kleppe, A. P. Jephcoat, and P. Macchi, "Putting pressure on aromaticity along with in situ experimental electron density of a molecular crystal," Nat. Commun. **7**, 10901 (2016).

[7] M. Chandrasekhar, S. Guha, and W. Graupner, "Squeezing organic conjugated molecules—What does one learn?," Adv. Mater. **13**, 613–618 (2001).

[8] M. Kato, M. Higashi, and Y. Taniguchi, "Effect of pressure on the internal rotation angle of biphenyl in carbon disulfide," J. Chem. Phys. **89**, 5417–5421 (1988).

[9] I. D. Brown, P. Klages, and A. Skowron, "Influence of pressure on the lengths of chemical bonds," Acta Crystallogr. B **59**, 439–448 (2003).

[10] P. Puschnig, C. Ambrosch-Draxl, G. Heimel, E. Zojer, R. Resel, G. Leising, M. Kriechbaum, and W. Graupner, "Pressure studies on the intermolecular interactions in biphenyl," Synth. Met. **116**, 327–331 (2001).

[11] A. Katrusiak, "High-pressure X-ray diffraction study of 2-methyl-1,3-cyclopentanedione crystals," High Pressure Res. **6**, 155–167 (1991).

[12] L. Cartz, S. R. Srinivasa, R. J. Riedner, J. D. Jorgensen, and T. G. Worlton, "Effect of pressure on bonding in black phosphorus," J. Chem. Phys. **71**, 1718–1721 (1979).

[13] E. Zurek and W. Grochala, "Predicting crystal structures and properties of matter under extreme conditions via quantum mechanics: The pressure is on," Phys. Chem. Chem. Phys. **17**, 2917–2934 (2015).

[14] P. Demontis, R. Lesar, and M. L. Klein, "New high-pressure phases of ice," Phys. Rev. Lett. **60**, 2284–2287 (1988).

[15] S. Nosé and M. L. Klein, "Constant pressure molecular dynamics for molecular systems," Mol. Phys. **50**, 1055–1076 (1983).

[16] M. Mugnai, G. Cardini, and V. Schettino, "Charge separation and polymerization of hydrocarbons at an ultrahigh pressure," Phys. Rev. B **70**, 020101 (2004).

[17] S. Imoto, P. Kibies, C. Rosin, R. Winter, S. M. Kast, and D. Marx, "Toward extreme biophysics: Deciphering the infrared response of biomolecular solutions at high pressures," Angew. Chem., Int. Ed. **55**, 9534–9538 (2016).

[18] D. Marx and J. Hutter, *Ab Initio Molecular Dynamics. Basic Theory and Advanced Methods*, 1st ed. (Cambridge University Press, Cambridge, UK, 2009).

[19] T. Stauch, "Quantum chemical modeling of molecules under pressure," Int. J. Quantum Chem. **2020**, e26208.

[20] R. Cammi, V. Verdolino, B. Mennucci, and J. Tomasi, "Towards the elaboration of a QM method to describe molecular solutes under the effect of a very high pressure," Chem. Phys. **344**, 135–141 (2008).

[21] R. Cammi, "New extension of the polarizable continuum model: Toward a quantum chemical description of chemical reactions at extreme high pressure," J. Comput. Chem. **36**, 2246–2259 (2015).

[22] B. Chen, R. Hoffmann, and R. Cammi, "The effect of pressure on organic reactions in fluids: A new theoretical perspective," Angew. Chem., Int. Ed. **56**, 11126–11142 (2017).

[23] R. Fukuda and K. Nakatani, "Quantum chemical study on the high-pressure effect for [4 + 4] retrocycloaddition of anthracene cyclophane photodimer," J. Phys. Chem. C **123**, 4493–4501 (2019).

[24] M. Pagliai, G. Cardini, and R. Cammi, "Vibrational frequencies of fullerenes C_{60} and C_{70} under pressure studied with a quantum chemical model including spatial confinement effect," J. Phys. Chem. A **118**, 5098–5111 (2014).

[25] R. Fukuda, M. Ehara, and R. Cammi, "Modeling molecular systems at extreme pressure by an extension of the polarizable continuum model (PCM) based on the symmetry-adapted cluster-configuration interaction (SAC-CI) method: Confined electronic excited states of furan as a test case," J. Chem. Theory Comput. **11**, 2063–2076 (2015).

[26] M. Rahm, R. Cammi, N. W. Ashcroft, and R. Hoffmann, "Squeezing all elements in the periodic table: Electron configuration and electronegativity of the atoms under compression," J. Am. Chem. Soc. **141**, 10254–10271 (2019).

[27] C. Caratelli, R. Cammi, R. Chelli, M. Pagliai, G. Cardini, and V. Schettino, "Insights on the realgar crystal under pressure from XP-PCM and periodic model calculations," J. Phys. Chem. A **121**, 8825–8834 (2017).

[28] T. Stauch and A. Dreuw, "Advances in quantum mechanochemistry: Electronic structure methods and force analysis," Chem. Rev. **116**, 14137–14180 (2016).

[29] G. Subramanian, N. Mathew, and J. Leiding, "A generalized force-modified potential energy surface for mechanochemical simulations," J. Chem. Phys. **143**, 134109 (2015).

[30] S. K. Jha, K. Brown, G. Todde, and G. Subramanian, "A mechanochemical study of the effects of compression on a Diels-Alder reaction," J. Chem. Phys. **145**, 074307 (2016).

[31] G. Todde, S. K. Jha, and G. Subramanian, "The effect of external forces on the initial dissociation of RDX (1,3,5-trinitro-1,3,5-triazine): A mechanochemical study," Int. J. Quantum Chem. **117**, e25426 (2017).

[32] M. T. Ong, J. Leiding, H. Tao, A. M. Virshup, and T. J. Martínez, "First principles dynamics and minimum energy pathways for mechanochemical ring opening of cyclobutene," J. Am. Chem. Soc. **131**, 6377–6379 (2009).

[33] T. Stauch, R. Chakraborty, and M. Head-Gordon, "Quantum chemical modeling of pressure-induced spin crossover in octahedral metal-ligand complexes," ChemPhysChem **20**, 2742–2747 (2019).

[34] P. Hohenberg and W. Kohn, "Inhomogeneous electron gas," Phys. Rev. **136**, 864–871 (1964).

[35] W. Kohn and L. J. Sham, "Self-consistent equations including exchange and correlation effects," Phys. Rev. **140**, 1133–1138 (1965).

[36] Y. Shao *et al.*, "Advances in molecular quantum chemistry contained in the Q-Chem 4 program package," Mol. Phys. **113**, 184–215 (2014).

[37] G. S. Kochhar, G. S. Heverly-Coulson, and N. J. Mosey, "Theoretical approaches for understanding the interplay between stress and chemical reactivity," Top. Curr. Chem. **369**, 37–96 (2015).

[38] A. W. Lange and J. M. Herbert, "Polarizable continuum reaction-field solvation models affording smooth potential energy surfaces," J. Phys. Chem. Lett. **1**, 556–561 (2010).

[39] M. Rahm, M. Ångqvist, J. M. Rahm, P. Erhart, and R. Cammi, "Non-bonded radii of the atoms under compression," ChemPhysChem (published online).

[40] A. Bondi, "van der Waals volumes and radii," J. Phys. Chem. **68**, 441–451 (1964).

[41] J. P. Perdew, K. Burke, and M. Ernzerhof, "Generalized gradient approximation made simple," Phys. Rev. Lett. **77**, 3865–3868 (1996).

[42] T. H. Dunning, "Gaussian basis sets for use in correlated molecular calculations. I. The atoms boron through neon and hydrogen," J. Chem. Phys. **90**, 1007–1023 (1989).

[43] A. D. Becke, "Density-functional exchange-energy approximation with correct asymptotic behavior," Phys. Rev. A **38**, 3098–3100 (1988).

[44] C. Lee, W. Yang, and R. G. Parr, "Development of the Colle-Salvetti correlation-energy formula into a functional of the electron density," Phys. Rev. B **37**, 785–789 (1988).

[45] A. D. Becke, "A new mixing of Hartree-Fock and local density-functional theories," J. Chem. Phys. **98**, 1372–1377 (1993).

[46] W. J. Hehre, R. Ditchfield, and J. A. Pople, "Self-consistent molecular orbital methods. XII. Further extensions of Gaussian-type basis sets for use in molecular orbital studies of organic molecules," J. Chem. Phys. **56**, 2257–2261 (1972).

[47] H. Liu, F. Wang, and X. Gong, "DFT studies on 7-nitrotetrazolo [1,5]furazano [4,5-b]pyridine 1-oxide: Crystal structure, detonation properties, sensitivity and effect of hydrostatic compression," Struct. Chem. **25**, 239–249 (2014).

[48] T. A. de Toledo, R. C. da Costa, R. R. F. Bento, and P. S. Pizani, "Hydrostatic pressure and temperature effect on the Raman spectra of the molecular crystal 2-amine-1,3,4-thiadiazole," J. Mol. Struct. **1156**, 127–135 (2018).

[49] F. Tassone, G. L. Chiarotti, R. Rousseau, S. Scandolo, and E. Tosatti, "Dimerization of CO_2 at high pressure and temperature," ChemPhysChem **6**, 1752–1756 (2005).

[50] T. Stauch and A. Dreuw, "Quantum chemical strain analysis for mechanochemical processes," Acc. Chem. Res. **50**, 1041–1048 (2017).